www.clinicalimagingscience.org

ScientificScholar®
Knowledge is power
Publisher of Scientific Journals

Journal of Clinical Imaging Science

Original Research

Techniques for Improving Ultrasound Visualization of Biopsy Markers in Axillary Lymph Nodes

Christine Lee[1], Chenyun Zhou[2], Brenda Hyde[3], Pengfei Song[4], Nicholas Hangiandreou[5]

[1]Department of Radiology, Division of Breast Imaging and Intervention, Mayo Clinic, [5]Department of Radiology, Division of Medical Physics, Mayo Clinic, Rochester, [3]Consulting Radiologists Ltd., Edina, MN, [2]Department of Ultrasound, West China Hospital of Sichuan University, Chengdu, Sichuan, China, [4]Department of Electrical and Computer Engineering, University of Illinois at Urbana-Champaign, Urbana, IL.

***Corresponding author:**
Christine Lee,
Department of Radiology,
Division of Breast Imaging
and Intervention, Mayo Clinic,
Mayo Clinic 200 First St, SW,
Rochester - 55905, Minnesota,
United States.

lee.christine@mayo.edu

Received : 21 January 2020
Accepted : 03 April 2020
Published : 18 April 2020

DOI
10.25259/JCIS_9_2020

Quick Response Code:

ABSTRACT

Objective: Biopsy markers are often placed into biopsy-proven metastatic axillary lymph nodes to ensure later accurate node excision. Ultrasound is the preferred imaging modality in the axilla. However, sonographic identification of biopsy markers after neoadjuvant therapy can be challenging. This is due to poor conspicuity relative to surrounding parenchymal interfaces, treatment-related alteration of malignant morphology during neoadjuvant chemotherapy, or extrusion of the marker from the target. To the authors' knowledge, the literature provides no recommendations for ultrasound scanning parameters that improve the detection of biopsy markers. The purpose of this manuscript is 3-fold: (1) To determine scanning parameters that improve sonographic conspicuity of biopsy markers in a phantom and cadaver model; (2) to implement these scanning parameters in the clinical setting; and (3) to provide strategies that might increase the likelihood of successful ultrasound detection of biopsy markers in breast imaging practices.

Materials and Methods: An *ex vivo* study was performed using a phantom designed to simulate the heterogeneity of normal mammary or axillary soft tissues. A selection of available biopsy markers was deployed into this phantom and ultrasound (GE LOGIQ E9) was performed. Scanning parameters were adjusted to optimize marker conspicuity. For the cadaver study, the biopsy markers were deployed using ultrasound guidance into axillary lymph nodes of a female cadaver. Adjustments in transducer frequency, dynamic range, cross-beam (spatial compound imaging), beam steering, speckle reduction imaging, harmonic imaging, colorization, and speed of sound were evaluated. Settings that improved marker detection were used clinically for a year.

Results: Sonographic scanning settings that improved biopsy marker conspicuity included increasing transducer frequency, decreasing dynamic range, setting cross-beam to medium hybrid, turning on beam steering, and setting speckle reduction imaging in the mid-range. There was no appreciable improvement with harmonic imaging, colorization, or speed of sound.

Conclusion: On a currently available clinical ultrasound scanning system, ultrasound scanning parameters can be adjusted to improve the conspicuity of biopsy markers. Overall, optimization requires a balance between techniques that clinically increase contrast (dynamic range, harmonic imaging, and steering) and those that minimize graininess (spatial compound imaging, speckle reduction imaging, and steering). Additional scanning and procedural strategies have been provided to improve the confidence of sonographic detection of biopsy markers closely associated with the intended target.

Keywords: Breast cancer, Axillary lymph node, Ultrasound, Localization, Biopsy clip or marker

INTRODUCTION

When it was determined that the false-negative rate of sentinel lymph node surgery in patients with node-positive breast cancer (T0-4, N1-2, and M0 [TNM classification]) could be reduced

by identifying and resecting the marked positive axillary lymph node,[1] pre-operative localization of the marked node became the practice at many medical facilities. Pre-operative localization of the marked node can be challenging, particularly after positive treatment response to neoadjuvant therapy. At this time, the positive axillary lymph node often becomes mammographically or sonographically occult, leaving only the biopsy marker in or near the site of the node.

Biopsy markers are made of either titanium, stainless steel, an alloy of titanium, and nickel, or ceramic and typically range from 1 mm (smallest dimension) to 8 mm (greatest dimension) [Table 1]. A myriad of marker conformations is commercially available, each describing visibility on ultrasound (US), mammograms, and magnetic resonance imaging (MRI), as well as minimal soft-tissue migration of the marker once it has been deployed.[2-4]

Despite mammographic conspicuity of all metallic biopsy markers, US is the imaging modality of choice in the axilla. Aside from using ionizing radiation, a mammographic approach can be technically challenging in the axilla, particularly when the marked positive node must be included between the mammographic plates. For many patients, this can be an uncomfortable position, making it difficult to perform mammographic- or tomosynthesis-guided localization. If the marked positive lymph node is located very far posteriorly, a mammographic technique may be prohibitive. For these reasons, breast radiologists prefer US-guided localizations of the marked lymph node. However, confidently identifying the marked positive lymph node by US after neoadjuvant chemotherapy can be challenging, if not impossible.

Two main factors contribute to the difficulties in detecting the marked lymph node after neoadjuvant chemotherapy. The first factor is poor marker conspicuity due to surrounding echogenic Cooper's ligaments, dense fibroglandular tissue, or shadowing tissue interfaces related to the heterogeneity of the breast parenchyma. The other factors are suspected extrusion or migration of the marker away from the positive lymph node as the lymph node normalizes during neoadjuvant chemotherapy. Both factors uniquely contribute to the complexity of US detection of the positive lymph node at the time of pre-operative localization.

Very little, if any, literature is available that describes ways to optimize sonographic visualization of the marker in an axillary lymph node, particularly after neoadjuvant chemotherapy. The purpose of this manuscript is to optimize sonographic scanning parameters for marker conspicuity in a phantom and cadaver model. A reflection on more than a year of clinically implementing these optimization trends is provided. Finally, a few helpful strategies are suggested, which might increase the likelihood of successfully identifying the marked lymph node by US in clinical practice.

MATERIALS AND METHODS

This study was approved by our Institutional Review Board and was compliant with the Health Insurance Portability and Accountability Act (HIPAA). The *ex vivo* section of this study involved (1) designing a reproducible phantom model that mimics normal mammary and axillary soft tissue and (2) sonographically evaluating biopsy markers used in our breast radiology practice, first in the phantom model and then in the cadaver model. The biopsy markers or clips used in this investigation were either expired or opened but never used; these included O-, cylinder-, top hat-, coil-, and U-shaped markers [Table 1]. The O-shaped and U-shaped markers are associated with resorbable packing or embedding material;[5] the coil-shaped clip with biodegradable hydrogel polymer; and the top hat-shaped marker with resorbable netting. Such surrounding material was removed, and the metallic clips were isolated for the *ex vivo* studies to simulate what generally remains in patients after months of neoadjuvant chemotherapy.

Eight clinically available US scanning parameters, frequency, dynamic range, cross-beam setting, beam steering, speckle reduction processing, harmonic imaging, colorization, and speed of sound, were adjusted to optimize conspicuity of the clip on a GE LOGIQ E9 US unit (GE Healthcare Inc., Wauwatosa, WI USA). The broad-spectrum linear matrix array transducer (ML6–15) is the probe most often used for breast USs, and this was the probe used for the cadaver study. For the phantom study, the 9L probe was also used. Time gain compensation, focusing, and output power were variably adjusted as in the clinical setting.

Phantom study

The phantom study began with the design and development of a phantom model that simulates mammary parenchyma on US. Grapefruit pulp provided heterogeneity suggestive of background breast parenchyma that would make finding a biopsy marker challenging [Figure 1]. Grapefruit pulp is difficult to maintain in form and difficult to preserve. Therefore, the recipe for a standard gel phantom was modified to include talcum powder or flour of varying amounts. The phantom was created with layers of molded gel (some with and without talcum powder or flour) and variably thick layers of paper towels/tissue [Figure 2]. A further modification which wrapped the gel pieces with cellophane and then stacked them randomly in a mold resulted in similar imaging features.

The O-, cylinder-, top hat-, coil-, and U-shaped markers were placed into one of the phantoms and scanned with an ML6–15 MHz probe using default settings that simulate the clinical environment.

Table 1: Selected available biopsy markers. For each of the biopsy markers, the measured size and manufacturer are provided.

Biopsy marker	Measured size (mm × mm)	Manufacturer information
O	1 × 2	SenoRx, Inc., Tempe, AZ, USA
Cylinder	1 × 3	Trimark, Hologic Inc., Marlborough, MA
Top hat	1 × 2	SecurMark, Hologic Inc., Marlborough, MA
Coil	1 × 2	Mammotome HydroMARK, Leica Biosystems, Wetzlar, Germany SenoMark UltraCor, Bard Biopsy, Tempe, AZ, USA
U	1 × 2–3	MammoMARK/CorMARK, Leica Biosystems, Wetzlar, Germany
Ribbon	1 × 3	Bard UltraClip, Tempe, AZ, USA
U	3 × 4	Tumark Professional U, Somatex Medical Technologies, Teltow, Germany
Vision	3 × 7	Tumark Vision, Somatex Medical Technologies, Teltow, Germany
Eye	2 × 8	Tumark Eye, Somatex Medical Technologies, Teltow, German

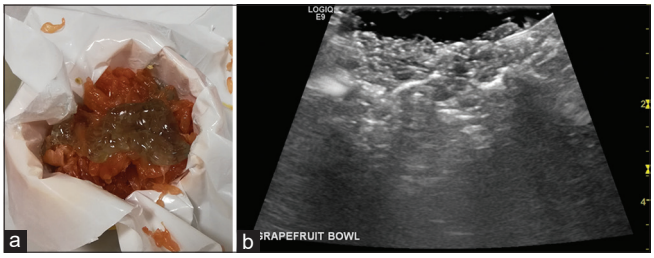

Figure 1: Grapefruit simulating mammary tissue on ultrasound (US). Pulp from a grapefruit was collected and placed in a container, and US gel was placed on top (a). The US image (b) shows heterogeneity and shadowing that mimics the tissue interfaces in mammary tissue.

Cadaver study

In collaboration with colleagues in the anatomy laboratory, a female cadaver with axillary lymph nodes was identified. The ribbon- and U-shaped markers were percutaneously deployed into the axillary nodes, and two radiologists (CL and BH) starting with the default biopsy preset mode adjusted the eight US scanning parameters described earlier until conspicuity of the marker was deemed optimal by consensus.

RESULTS

In the phantom study, the O- and U-shaped markers were essentially inconspicuous [Figure 3] with the O-shaped marker marginally more conspicuous than the U-shaped one. For the cadaver study, the adjustments to the eight scanning parameters of the default settings are summarized in Table 2, where additional figures are referenced.

DISCUSSION

Identifying marked axillary lymph nodes for radioactive I-125 seed localization after neoadjuvant therapy can be challenging for several reasons. These include altered morphology (normalization) of the treated lymph node, suspected extrusion of the marker from the lymph node, and poor sonographic conspicuity of the markers. This study reviewed modifications of several widely available scanning parameters during US evaluation of marked axillary lymph nodes to improve marker conspicuity and confidence of marker detection. Although the availability of cadavers with axillary lymph nodes only allowed for limited evaluations, it did provide insight and the realization that some of the

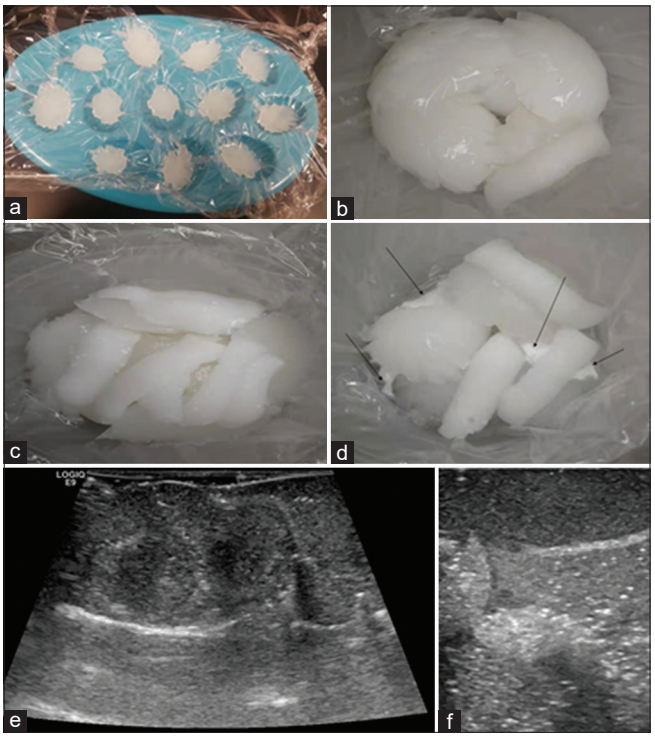

Figure 2: Construction of a phantom that simulates normal mammary parenchyma on ultrasound (US). Using a standard recipe for making gel phantoms, the material was poured into a cellophane-covered mold with shallow half-egg shapes (a). These gel molds were layered (b) along with other layers of phantom material mixed with either talcum powder containing $Ca_3(PO_4)_2$ or ZnO or mixed with 1 g flour (c). Layers of paper towels of variable thicknesses (d, layers) were layered in between the gel layers. US shows heterogeneous echotexture (e,f) that simulates mammary parenchyma.

Table 2: Optimization of ultrasound parameters in a cadaver model. For each parameter, the default settings in biopsy mode are shown followed by the adjustments made. The preference is then noted, and an example is provided in the form of a figure.

Parameter	Default biopsy mode setting	Adjustment from default biopsy mode	Preference	Example
Frequency	11 MHz	9 MHz, 13 MHz, 15 MHz	Higher frequencies	Figure 4
Dynamic range	72 dB	41 dB, 48 dB, 69 dB	69 dB	Figure 5
Cross-beam (spatial compound imaging)	Low mean	Medium hybrid	Medium hybrid	Figure 6
Beam steering	Disabled	Enabled and in direction perpendicular to orientation of the marker	On	Figure 7
Speckle reduction imaging	4	0, 3, 5	3	Figure 8
Harmonic imaging	Disabled	Enabled	No preference	Figure 9
Speed of sound	1540 m/s	1420 m/s	No preference	None
Color	Gray scale	Tinted	No preference	None

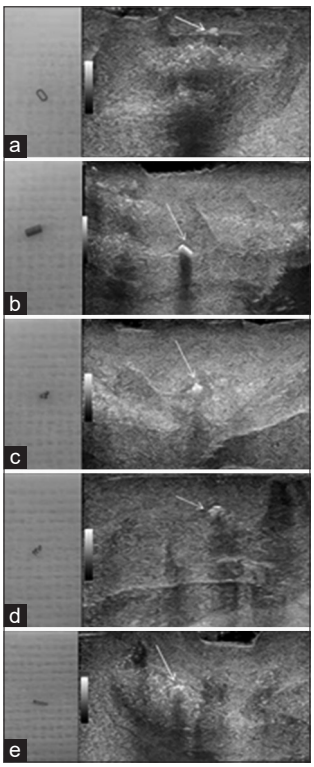

Figure 3: Biopsy markers in a phantom. The O-shaped (a) and U-shaped (e) markers were less conspicuous than the cylinder (b), top hat (c), and coil-shaped (d) markers on ultrasound (US) using default scanning parameters for breast US and an ML6-18 MHz probe.

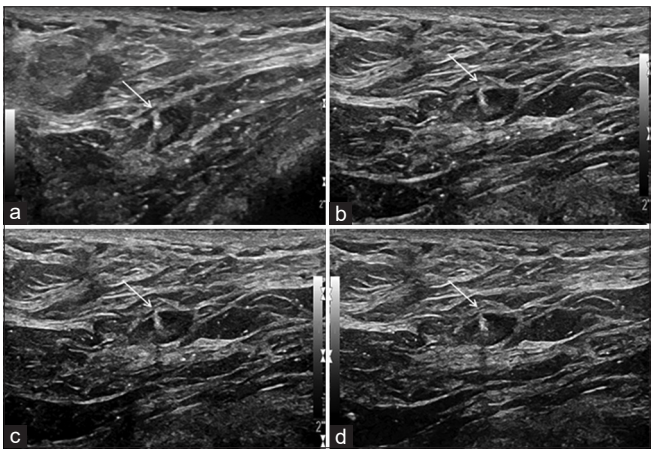

Figure 4: Optimization of frequency in a cadaver model. Ultrasound (US) transducers are specified by their center frequencies but operate within a range of frequencies or bandwidth. Breast US typically uses a few transducers to provide frequencies in the 7 MHz–18 MHz range. Although higher frequencies offer higher resolution, the depth of penetration through soft tissues is lower, making higher frequencies better for superficial imaging and lower frequency better for imaging deeper soft tissues. The biopsy marker is an echogenic focus in each image (arrow). The default biopsy mode uses 11 MHz (a). The adjustments were 9 MHz (b), 13 MHz (c), and 15 MHz (d). The preferred frequencies for this case were 13 MHz and 15 MHz, all higher than the default. This could be related to the depth of the target for this case. As a rough approximation, the depth of penetration can be estimated by (60 cm MHz)/f, where f is in MHz. Using this rough calculation in this particular case, a 60 MHz center frequency transducer might be helpful for this depth of penetration. However, this rough calculation is affected by the attenuation coefficient, an indicator of acoustic loss, which can be quite variable depending on the insonated soft tissues.[12] In this case, increasing the frequency narrows the width of the ultrasound beam which makes it more and more difficult to get around the marker and thus makes the shadow prominent.

expected optimization trends were occasionally not the ones preferred. While the preference of higher frequencies, for example, made theoretical sense based on physics, other adjustments were more counter intuitive. For instance, in this study, there was no preference when using harmonic imaging. This seems to support studies which have shown that harmonic imaging provided limited value in needle visualization in the breast.[6,7] There is also an interplay between dynamic range, spatial compound imaging, speckle reduction imaging, and harmonic imaging that need to be

Table 3: Strategies that can improve confidence in detecting or confirming the marked positive node by US. The left-hand column lists strategies that may help to ensure later detection of the marked positive lymph node after neoadjuvant chemotherapy. The right-hand column lists strategies that may be helpful at the time of localization when the positive lymph node has a normal imaging appearance or is not readily seen, and the marker is not easily detected.

At the time of fine-needle aspiration or marker placement when the abnormal lymph node is easily detected, or anytime during follow-up US when the marked node is well seen before pre-operative localization	**At the time of pre-operative localization**
1. Field of view Include a cine clip of the abnormal lymph node with a larger field of view or with virtual convex, paying particular attention to include adjacent anatomic landmarks; more than one orientation may be helpful. The aim is to ensure the reproducibility of scanning orientation and transducer placement. 2. Reporting/annotating Consider reporting or annotating on an image frame the location of the marked lymph node relative to a unique skin finding (e.g., freckle, mole, and skin tag) or distance from the nipple. 3. Indelible skin mark Consider making a tattoo dot at the location of the lymph node. This can be performed as a clean technique with a drop of SteriTatt Black Ink Dropper (Klarity Medical Products, Newark, OH, USA) on the skin, followed by gentle insertion of a 21G or 20G needle through the ink and just under the skin surface. The remainder of the ink is wiped away, leaving a small tattoo dot.	1. Positioning Ask the patient if she is similarly positioned compared to previous axillary ultrasound examinations; consider adjusting the patient's arm during the scan. 2. Transducer pressure Consider increasing transducer pressure; this is particularly helpful to bring deeper marked nodes into the near-field. 3. Procedural confirmation At the time of obtaining local anesthesia, attempt to inject lidocaine or sterile saline immediately around the suspected marker, or attempt to tap on the marker with the needle tip.

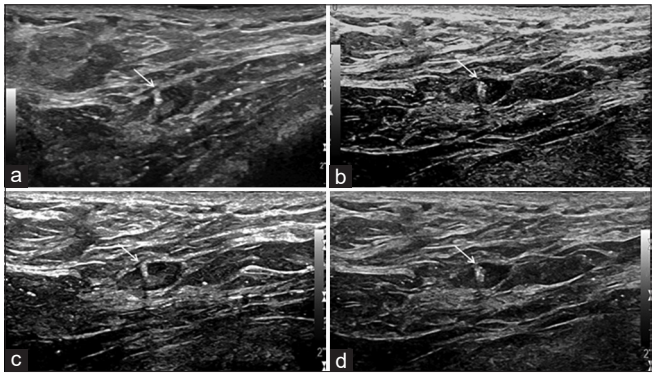

Figure 5: Optimization of dynamic range in a cadaver model. The dynamic range describes the range in decibels (dB) between the largest and smallest signal at any given processing step. It is roughly analogous to how wide or narrow the window is on a radiograph or computed tomography. A wide dynamic range has more shades of gray, less contrast, and makes the image appear smoother.[13] A narrow dynamic range has fewer shades of gray, more contrast, and makes the image appear grainy. The biopsy marker is an echogenic focus in each image (arrow). The default biopsy mode is 72 dB (a). The adjustments were 41 dB (b), 48 dB (c), and 69 dB (d). The preferred dynamic range was 69 dB. The increased contrast associated with the narrower dynamic range seemed to make it harder to distinguish the hyperechoic marker from adjacent hyperechoic Cooper's ligaments and parenchymal interfaces.

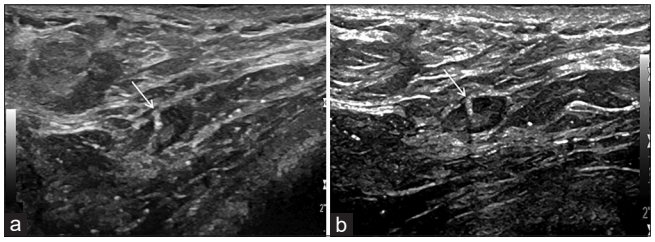

Figure 6: Optimization of cross-beam in a cadaver model. Cross-beam, also called spatial compound imaging, averages three or more echoes from different steering angles into a single image.[14,15] This is accomplished when the probe sends multiple interrogation beams at various angles through the same tissue instead of at a single angle as in conventional B-mode imaging. Spatial compound imaging or cross-beam techniques have been shown to eliminate noise, graininess, and refractive shadows,[14,16] creating improved edge detail and contrast. The use of cross-beam slows down the frame rate (due to more lines of sight) and is variably helpful clinically for either very superficial or very deep structures in the breast. The biopsy marker is an echogenic focus in each image (arrow). The default biopsy mode is cross-beam low mean (a), which means that separate sets of pulse or echo data are acquired for a low number of angles and that the averages of the detected echo signals from each angle are then assigned to the compound image pixel values. The adjustment to cross-beam medium hybrid (b) was preferred for this case. This means that a medium number of angles were used to acquire the data, and a hybrid calculation between mean and max (determined by the vendor) was used to determine the compound image pixel values.

explored for each case, given the variations in depth of the marked lymph node, the type of marker, and the conspicuity of the positive lymph node after neoadjuvant chemotherapy. For the cadaver model, sonographic optimization techniques included increasing transducer frequency, slightly decreasing dynamic range, setting cross-beam to medium hybrid, turning on beam steering, and setting speckle reduction imaging to mid-range. Different vendors have slight

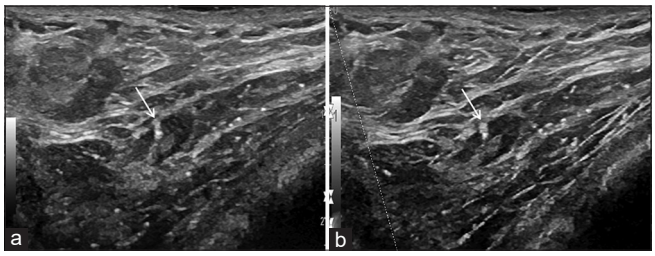

Figure 7: Optimization using steering in a cadaver model. Beam steering is a form of compound imaging, in which the beam is directed perpendicular to a biopsy needle or other object of interest, such as a marker. The result is that the object appears brighter. The biopsy marker is an echogenic focus in each image (arrow). The default biopsy mode is without beam steering (a). The preferred adjustment is with beam steering (b). In this case, it is presumed that beam steering is perpendicular to the marker.

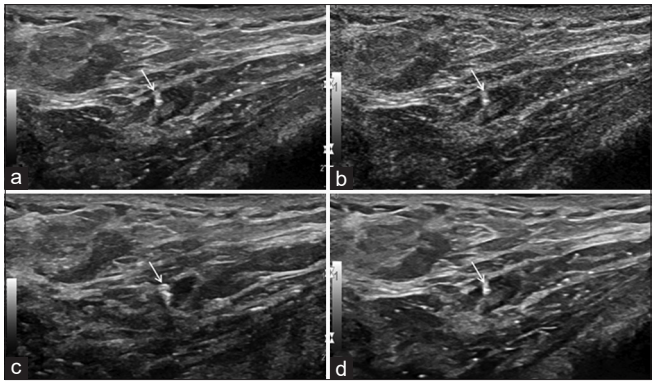

Figure 8: Optimization of speckle reduction index in a cadaver model. Speckle is an intrinsic artifact which degrades ultrasound image quality. Speckle reduction imaging (SRI) uses image processing techniques to remove speckle.[17,18] SRI will generally make the image appear smoother. Low SRI removes a small amount of artifact, while high SRI may look over-processed. Higher SRI is associated with a slower frame rate. The biopsy marker is an echogenic focus in each image (arrow). The default biopsy mode has a speckle reduction set at 4. The adjustments are SRI = 0 (B), SRI = 3 (C), and SRI = 5 (D). The most preferred of the three was SRI = 3.

variations that instantiate the parameters tested, and these will need to be optimized accordingly.

A limitation of this study is that any material surrounding the metallic marker was removed. For some markers, the surrounding material may be the very feature that makes it sonographically conspicuous. The biodegradability of materials surrounding the metallic components varies, so markers identified indirectly by said materials may or may not be detectable months after neoadjuvant chemotherapy.

After more than a year of implementing these US techniques optimized for marker detection in the clinical setting, successful detection seems to be a balance between techniques that increase contrast and those that minimize graininess. Vocal fremitus, elastography, Doppler, and power

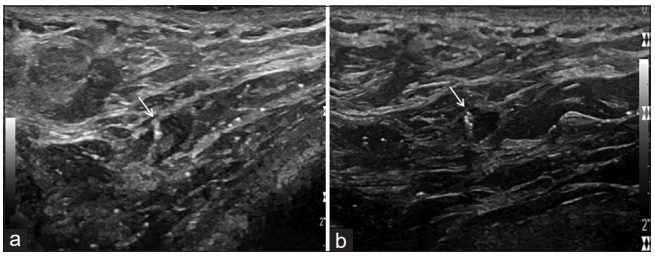

Figure 9: Optimization of harmonic imaging in a cadaver model. Harmonic imaging processes the second harmonic signal generated during insonation.[13,19] Advantages of harmonic imaging include increased signal-to-noise ratio, which makes it occasionally helpful in the breast to characterize near-field, small, isoechoic masses, and far-field entities. The biopsy marker is an echogenic focus in each image (arrow). Harmonic imaging is disabled in the default biopsy mode setting (a). There was no preference between turning harmonic imaging off (a) or on (b) for this case. Harmonic imaging also improves resolution (2× imaging frequency), which can be another observation here that improving spatial resolution did not really help – it may be because we are improving the resolution of everything by an equal amount.

reduction provided no additional improvement in marker detection. However, a few strategies seem to improve the likelihood of detecting or confirming the marked positive node by US, and it starts from the time of the fine-needle aspiration and marker placement [Table 3].

When US is unsuccessful in identifying a marked axillary node, alternative imaging guidance such as CT or tomosynthesis can be considered.[8-10] A limited selection of biopsy markers with similar imaging characteristics was used for the cadaver model. There are a variety of biopsy markers on the market, and a large number have been reviewed as options for localization of axillary lymph nodes.[11] Hygroscopic markers such as the HydroMARK coil-shaped markers (Mammotome HydroMARK, Norderstedt, Germany) seemed hopeful for improving sonographic detection, but aside from challenging detectability over time and migration or extrusion of the marker, there were initially, at our institution, concerns of false positives at the time of surgical pathology. In addition, non-wire localization techniques continue to explore their roles as biopsy markers to potentially obviate the localization step; these techniques include non-radioactive signaling sources such as iron particles (Magseed, Sentimag, Leica Biosystems, Wetzlar, Germany), radar (Savi Scout, Cianna Medical, Aliso Viejo, CA, USA), and radiofrequency tagging (LOCalizer, Faxitron, Tucson, AZ, USA).[11]

In the meantime, non-ionizing features, patient comfort, and costs make US the preferred imaging modality for identifying a marked axillary lymph node. There are several currently available US scanning parameters that can be explored and tweaked to improve the conspicuity of the marked node, and it may take extra time to determine the optimal setting for

each case. In addition, there are also clinical strategies that can be taken to improve the chances of detecting the marked positive lymph node.

CONCLUSION

Ultrasound scanning parameters can be adjusted to improve the conspicuity of biopsy markers. Overall, optimization requires a balance between techniques that increase contrast (dynamic range, harmonic imaging, and steering) and those that minimize graininess (spatial compound imaging, speckle reduction imaging, and steering). Additional scanning and procedural strategies can improve the confidence of sonographic detection of biopsy markers associated with the intended target.

Acknowledgments

The authors would like to acknowledge Rebecca L. Higgins, RT, RDMS, and Emily Smith, RVT, RDMS, for their assistance with US scanning parameter adjustments and insight, and Lyndsay Viers, M.D., for her efforts and assistance with obtaining IRB approval.

The authors would also like to acknowledge the assistance and support of Karen Mills, CST, Terry Regnier, and Shaun Heath from the Department of Anatomy. Our sincerest gratitude and respect go to the generosity and hopes of patients who donate their bodies for the advancement of medical practice.

Declaration of patient consent

Patient's consent not required as there are no patients in this study.

Financial support and sponsorship

Nil.

Conflicts of interest

There are no conflicts of interest.

REFERENCES

1. Boughey JC, Ballman KV, Le-Petross HT, McCall LM, Mittendorf EA, Ahrendt GM, *et al*. Identification and resection of clipped node decreases the false-negative rate of sentinel lymph node surgery in patients presenting with node-positive breast cancer (T0-T4, N1-N2) who receive neoadjuvant chemotherapy: Results from ACOSOG Z1071 (Alliance). Ann Surg 2016;263:802-7.
2. Pinkney DM, Mychajlowycz M, Shah BA. A prospective comparative study to evaluate the displacement of four commercially available breast biopsy markers. Br J Radiol 2016;89:20160149.
3. Plecha D, Bai S, Patterson H, Thompson C, Shenk R. Improving the accuracy of axillary lymph node surgery in breast cancer with ultrasound-guided wire localization of biopsy proven metastatic lymph nodes. Ann Surg Oncol 2015;22:4241-6.
4. Esserman LE, Cura MA, DaCosta D. Recognizing pitfalls in early and late migration of clip markers after imaging-guided directional vacuum-assisted biopsy. Radiographics 2004;24:147-56.
5. Reisenbichler E. Breast Biopsy Marking Devices. California: Pathology Outlinescom. Inc.; 2020.
6. Mesurolle B, Bining HJ, El Khoury M, Barhdadi A, Kao E. Contribution of tissue harmonic imaging and frequency compound imaging in interventional breast sonography. J Ultrasound Med 2006;25:845-55.
7. Szopinski KT, Pajk AM, Wysocki M, Amy D, Szopinska M, Jakubowski W. Tissue harmonic imaging: Utility in breast sonography. J Ultrasound Med 2003;22:479-87; quiz 88-9.
8. Samreen N, Lee CU, Bhatt AA. Nonconventional options for tumor localization in breast and axillary lymph nodes: A pictorial how-to. J Clin Imaging Sci 2018;8:54.
9. Choudhery S, Simmons C, Harper L, Lee CU. Tomosynthesis-guided needle localization of breast and axillary lesions: Our initial experience. AJR Am J Roentgenol 2019;212:943-6.
10. Trinh L, Miyake KK, Dirbas FM, Kothary N, Horst KC, Lipson JA, *et al*. CT-guided wire localization for involved axillary lymph nodes after neo-adjuvant chemotherapy in patients with initially node-positive breast cancer. Breast J 2016;22:390-6.
11. Woods RW, Camp MS, Durr NJ, Harvey SC. A review of options for localization of axillary lymph nodes in the treatment of invasive breast cancer. Acad Radiol 2018;26:805-19.
12. Szabo TL, Lewin PA. Ultrasound transducer selection in clinical imaging practice. J Ultrasound Med 2013;32:573-82.
13. Hangiandreou NJ. AAPM/RSNA physics tutorial for residents. Topics in US: B-mode US: Basic concepts and new technology. Radiographics 2003;23:1019-33.
14. Entrekin RR, Porter BA, Sillesen HH, Wong AD, Cooperberg PL, Fix CH. Real-time spatial compound imaging: Application to breast, vascular, and musculoskeletal ultrasound. Semin Ultrasound CT MR 2001;22:50-64.
15. Lin DC, Nazarian LN, O'Kane PL, McShane JM, Parker L, Merritt CR. Advantages of real-time spatial compound sonography of the musculoskeletal system versus conventional sonography. AJR Am J Roentgenol 2002;179:1629-31.
16. Weng L, Tirumalai AP, Lowery CM, Nock LF, Gustafson DE, Von Behren OL, *et al*. US extended-field-of-view imaging technology. Radiology 1997;203:877-80.
17. Liasis N, Klonaris C, Katsargyris A, Georgopoulos S, Labropoulos N, Tsigris C, *et al*. The use of speckle reduction imaging (SRI) ultrasound in the characterization of carotid artery plaques. Eur J Radiol 2008;65:427-33.
18. Wu S, Zhu Q, Xie Y. Evaluation of various speckle reduction filters on medical ultrasound images. Conf Proc IEEE Eng Med Biol Soc 2013;2013:1148-51.
19. Anvari A, Forsberg F, Samir AE. A primer on the physical principles of tissue harmonic imaging. Radiographics 2015;35:1955-64.

How to cite this article: Lee C, Zhou C, Hyde B, Song P, Hangiandreou N. Techniques for Improving Ultrasound Visualization of Biopsy Markers in Axillary Lymph Nodes. J Clin Imaging Sci 2020;10:21.